

NISTIR 7968

A Spectral Analytic Method for Fingerprint Image Sample Rate Estimation

John M. Libert
Shahram Orandi
John D. Grantham
Michael D. Garris

<http://dx.doi.org/10.6028/NIST.IR.7968>

NIST
National Institute of
Standards and Technology
U.S. Department of Commerce

NISTIR 7968

A Spectral Analytic Method for Fingerprint Image Sample Rate Estimation

John M. Libert
Shahram Orandi
John D. Grantham
Michael D. Garris

*Information Access Division
Information Technology Laboratory*

<http://dx.doi.org/10.6028/NIST.IR.7968>

February 2014



U.S. Department of Commerce
Penny Pritzker, Secretary

National Institute of Standards and Technology
Patrick D. Gallagher, Under Secretary of Commerce for Standards and Technology and Director

Table of Contents

1.	INTRODUCTION	1
2.	INVESTIGATIVE GOALS	2
3.	METHOD	2
3.1.	IMAGE DATA	2
3.1.1.	Model Development.....	2
3.1.2.	Model Testing.....	2
3.2.	SIVV PROCESSING.....	3
3.3.	PREDICTIVE REGRESSION MODEL.....	6
3.4.	UNCERTAINTY ANALYSIS.....	9
3.5.	PREDICTION RESULTS.....	11
4.	DISCUSSION OF RESULTS	13
5.	CONCLUSIONS	14
6.	REFERENCES	15

List of Tables

Table 1 Model parameter values and uncertainties	9
Table 2 Expanded Uncertainty for sample rates predicted by SIVV frequency.....	10

List of Figures

Figure 1 - Example of 10-print Card Utilized in this Study with Finger Numbers Annotated.....	3
Figure 2 - Fingerprint image digitized at 1000 ppi (995 x 1090 pixels).....	4
Figure 3 - Fingerprint image from fig. 2 resampled at 500 ppi (498 x 545 pixels) using bicubic interpolation. The spectral features are shifted by factor of 2 in frequency.....	5
Figure 4 - Peak Frequency of Strongest Peak as Detected by SIVV (f_1) vs. Image Sample Rate (sr).....	6
Figure 5 Fitted model predictions plotted over observed data. Frequency measurements are shown in relation to ground truth sample rates.	7
Figure 6 Weighted residuals (observed- predicted frequency)	8
Figure 7 Illustration of prediction of sample rate using the model with $\pm U$ shown as a red bar on the abscissa. The frequency measurements are plotted against the ground truth sample rates.....	11
Figure 8 Prediction accuracy within specified error thresholds SD27A cardscan, N= 24704.....	12
Figure 9 Prediction accuracy within specified error thresholds LAC livescan, N= 23198	13

ACKNOWLEDGEMENTS

The authors wish to give special thanks to the following individuals and organizations for their support of this work:

Federal Bureau of Investigation for all their support

T.J. Smith and the LA County Sheriff's Department

William F. Guthrie in the Statistical Engineering Division at NIST-ITL

DISCLAIMER

Specific hardware and software products identified in this report were used in order to perform evaluations. In no case does identification of any commercial product imply endorsement by the National Institute of Standards and Technology, nor does it imply that the products and equipment identified are necessarily the best available for the purpose.

Abstract

This study examines the use of the NIST Spectral Image Validation and Verification (SIVV) metric for the application of detecting the sample rate of a given fingerprint digital image. SIVV operates by reducing an input image to a 1-dimensional power spectrum that makes explicit the characteristic ridge structure of the fingerprint that on a global basis differentiates it from most other images. The magnitude of the distinctive spectral feature, which is related directly to the distinctness of the level 1 ridge detail, provides a primary diagnostic indicator of the presence of a fingerprint image. The location of the detected peak corresponding to the level 1 ridge detail can be used as an estimator of the original sampling frequency of that image given the behavior of this peak at known sampling frequencies *a priori* versus the calculated shift of this peak on an image of unknown sampling rate. A statistical model is fit to frequency measurements of a sample of images scanned at various sample rates from 10-print fingerprint cards such that the model parameters can be applied to SIVV frequency values of a digital fingerprint of unknown sample rate to estimate the sample rate. Uncertainty analysis is used to compute 95 % confidence intervals for predictions of sample rate from frequency. The model is tested against sets of cardscan and livescan images.

Keywords: fingerprint; sample rate estimation; SIVV; spectral analysis; Spectral Image Validation and Verification

1. Introduction

Fingerprint matching or verification in a contemporary sense involves several key steps that range from acquiring a digital representation of a fingerprint image from a finger (capture phase), processing of that digital fingerprint image into a vectorized representation that is suitable for comparison purposes (characterization), and then ultimately comparing that vectorized representation to other candidate vectorized representations (matching). Characterization of a fingerprint image into a representation that is suitable for matching typically involves the detection of salient features of interest in the fingerprint image, while comparison of candidate match pairs establishes constellations of salient features that the pair of candidates have in common with the relative distance in vector spaces as an indicator of the similarity for the candidate pair. The process of matching is dependent on the relative spatial location of the salient features, therefore as a pre-requisite, a common spatial sampling rate is needed for candidate pairs of features to be compared accurately and effectively. A common sampling rate is typically established by stakeholders of a system through various standards such as the American National Standard for Information Systems / National Institute of Standards and Technology (ANSI/NIST) standard [1] and the Federal Bureau of Investigation Electronic Biometric Transmission Specification (FBI EBTS) standard [2] which currently dictate either 500 ppi¹ (19.7 pixels per millimeter) or 1000 ppi (39.4 pixels per millimeter) as the fingerprint spatial sampling rate². While standards and system service agreements can provide strict guidelines on sampling rate accuracy and tolerances in the capture phase, such agreements and standards may not be able to guarantee the on-going adherence to these guidelines. In addition, random variability in the sampling rate of images, arising from a variety of sources, including unforeseen system faults, may ultimately result in degradation of matching performance.

In 2009, NIST in collaboration with the FBI developed the Spectral Image Validation and Verification (SIVV) utility. SIVV operates by reducing an input image to a 1-dimensional power spectrum that makes explicit the characteristic ridge structure of the fingerprint that on a global basis differentiates it from most other images. The magnitude of the distinctive spectral feature, related directly to the distinctness of the level 1 ridge flow, provides a primary diagnostic indicator of the presence of a fingerprint image as documented in NISTIR-7599 [3]. The frequency of the spectral feature also provides a novel secondary classification metric, which on a coarse level, indicates the sample rate of the fingerprint image. The study outlined here examines the spectral features extracted by SIVV and looks at the effectiveness of using this spectral footprint from a fingerprint to establish the original sample rate of the fingerprint which can be used to detect sampling rate anomalies as well as take mitigating action in fingerprint comparison.

¹ Resolution values for friction ridge imagery are specified in pixels per inch (ppi) throughout this document. This is based on widely used specification guidelines for such imagery and is accepted as common nomenclature within the industry. SI units for these will be presented only once.

² Other terms include image resolution, spatial resolution, and pixel spacing.

2. Investigative Goals

This study attempts to explore and validate application of the NIST SIVV metric for estimation of fingerprint image sample rate. Specific objectives include:

1. Development of a predictive statistical model by which the spatial sampling rate from a fingerprint image of unknown spatial characteristics may be predicted using the NIST SIVV algorithm.
2. Application of the predictive statistical model to images not included in development of the model to test the predictive performance of the model for a range of differences between actual and predicted sample rates.

3. Method

3.1. Image Data

3.1.1. Model Development

A dataset was constructed by sampling four standard FBI 10-print fingerprint cards, with twelve images per card. Prints #1 to #10 are rolled impressions of right and left hands. Prints #11 and #12 are flat impressions of the right and left thumbs (see Figure 1). The "slap-four" impressions also shown in Figure 1 were not used. Each full card was scanned at multiple sample rates ranging from 100 ppi to 2400 ppi at increments of 50 ppi, yielding 47 different sample rates. Fingerprint cards were scanned using an Epson 4990³ flatbed scanner. Individual fingerprint images were segmented from the full card scans using identical bounding coordinates. Only the rolled impressions of the 10 fingers, #1 through #10, and the flat impressions of both thumbs, #11 and #12 were included. This yielded a suite of 2256 fingerprint images for use in developing a model.

3.1.2. Model Testing

This dataset is a subset of fingerprint impressions taken from each of the fingerprint cards digitized to form NIST Special Database SD27⁴ [11]. This subset consisted of 2484 images scanned from standard FBI 10-print cards at 2000 ppi. These images consisted of 12 fingerprint impressions, as described above, for each of 207 subjects.

³ An Federal Bureau of Investigation (FBI) Appendix F [2] certified flatbed scanner

⁴ The SD27 dataset is described in [11]. We actually used images designated SD27A, a rescanning of the original 10-print cards at 500 ppi, 1000 ppi, and 2000 ppi.



Figure 1 - Example of 10-print Card Utilized in this Study with Finger Numbers Annotated

In the absence of a large number of fingerprints scanned at a variety of sample rates, we constructed a large test dataset by resampling fingerprint images scanned at 2000 ppi from the fingerprint cards as described above. Thus each of the 2000 ppi source images is resized via bicubic interpolation resampling with anti-aliasing (low-pass) filtering to simulate acquisition at the additional lower sample rates 1800 ppi, 1600 ppi, 1400 ppi, 1200 ppi, 1000 ppi, 800 ppi, 600 ppi, 400 ppi, and 200 ppi. This procedure yielded a test dataset consisting of 24 770 fingerprint images.

To examine the model against livescan fingerprints, we used a set of images provided by Los Angeles County, CA, referred to as LAC. These were acquired using a livescan device, the Identix TouchPrint 5800 (Appendix F certified). Fingerprints #1 to #10 are rolled and #11 and #12 are flat prints of the thumbs. As these were acquired at 1000 ppi, we followed the procedure described above to generate copies of each image at additional sample rates, 900 ppi, 800 ppi, 700 ppi, 600 ppi, 500 ppi, 400 ppi, 300 pi, 200 ppi, and 100 ppi. As with the SD27A dataset, only impressions #1 to #12 were used.

3.2. SIVV Processing

The NIST Spectral image Validation/Verification (SIVV) utility [3][4] was developed originally as a means to automatically identify non-fingerprint images or poor quality fingerprint images in large databases. It also proved useful as an image fidelity metric where it was employed in a number of JPEG 2000 fingerprint image compression studies [5][6][7][8][9][10]. In [3], Libert, *et. al.* we indicated potential use as a coarse classifier to differentiate fingerprint image sample rates, particularly 500 ppi and 1000 ppi.

For the present study, we employ the SIVV utility as implemented in the release 4.2.0 of the NIST Biometric Image Software (NBIS) [4]. Among the various outputs of the SIVV algorithm, we utilize the output that corresponds to the center frequency of the strongest peak in the measured spectrum (hereafter referred to simply as “peak frequency”). Prior experience with the SIVV tool has shown that this peak corresponds

to the level 1 ridge structure of a fingerprint which is the dominant frequency element in a typical fingerprint image. It was recognized in [3] that the frequency position of this peak shifts toward the high frequency as the sample rate is reduced. We note that this effect is actually an artifact of the scaling applied to the frequency spectrum by the SIVV algorithm rather than an actual measure of the ridge frequency⁵. Inspection of Figure 2 and Figure 3 illustrates the displacement of the dominant peak as sample rate is reduced from 1000 ppi to 500 ppi for the source image. Note also the broadening of the peak at the lower sample rate.

Due to normal anthropometric variance in the human finger ridge structure such frequency values should not be interpreted literally as ridge frequency of the fingerprint image as there is no such fixed frequency for the level 1 ridge structure of a human finger. It is hypothesized here that the systematic shift in the expected peak position could be used as an indicator or estimator of the sample rate of a given fingerprint image if a functional relationship between peak frequency and sampling rate could be established.

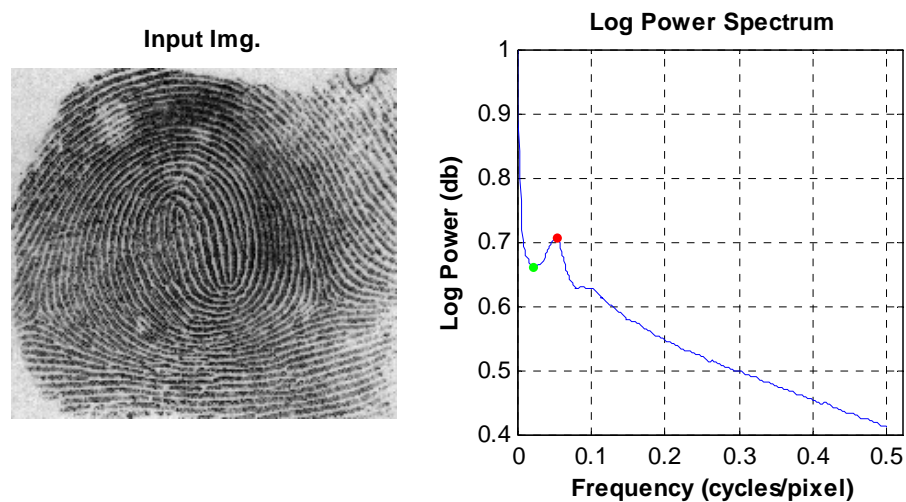


Figure 2 - Fingerprint image digitized at 1000 ppi (995 x 1090 pixels).

⁵ Expressed in cycles/pixel, the frequencies zero to 0.5 cycles/pixel are scaled to $\frac{1}{2}$ of the smallest dimension of the 2D power spectrum. The effect is to stretch out the spectrum of an image of lower sample rate relative to one of higher sample rate, pushing the location of the peak corresponding to the fingerprint ridge pattern toward the high frequency.

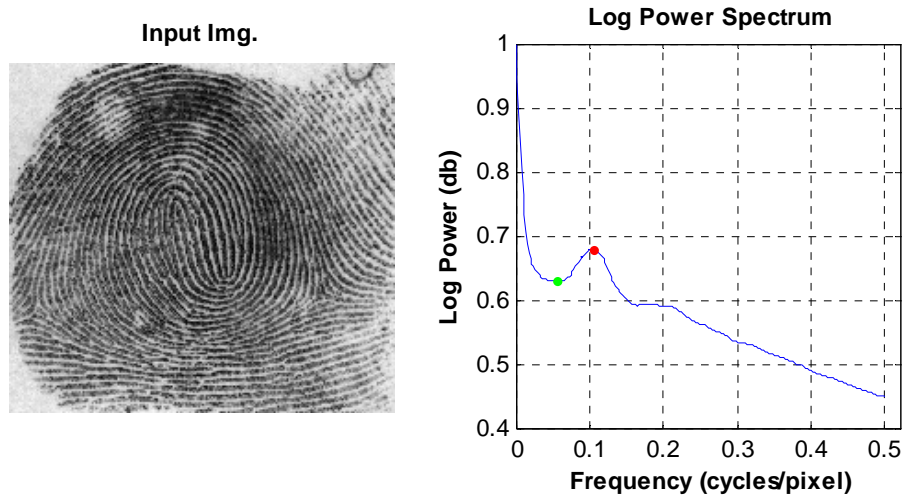


Figure 3 - Fingerprint image from fig. 2 resampled at 500 ppi (498 x 545 pixels) using bicubic interpolation. The spectral features are shifted by factor of 2 in frequency.

Each of the datasets described in section 3.1 were processed with the SIVV utility, recording the center frequency of the dominant spectral peak for each image. Then the training dataset was used to develop a regression model with which to predict the sample rate for the images of the test dataset.

3.3. Predictive Regression Model

Figure 4 below displays a scatter plot of the detected peak frequencies (using SIVV) for each of the test images (ordinate) against the ground-truth sample rates of the original digital fingerprint impression.

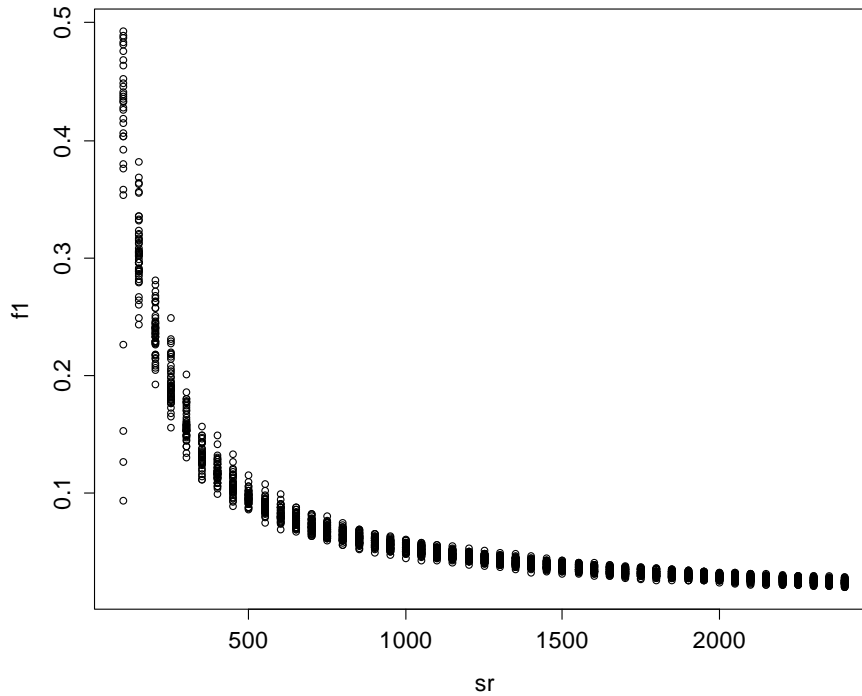


Figure 4 - Peak Frequency of Strongest Peak as Detected by SIVV (f_1) vs. Image Sample Rate (sr)

Observing this pattern to be of the general form, $y = k/x$, we chose to model this using a function of the form

$$frequency = \beta_0 + \beta_1 \left(\frac{1}{sample\ rate} \right) + \varepsilon \quad (1)$$

where *frequency* refers to the center frequency of the dominant peak of the SIVV spectrum (in cycles/pixel) and *sample rate* (in pixels/inch) to the sampling interval used in acquiring the digital fingerprint image.

We apply a linear model that uses an least squares algorithm [12][13] implemented in the **R** software package [14]. Additional data preparation employed functions developed using MATLAB® [15] software. Because the variance of frequency values is not uniform across all sample rates, we weight the cases by variance of frequency determined for each sample rate grouping using a smoothed version of the sample variances at each sampling rate shown in equation (2).

$$w_{i,k} = \frac{1}{\text{var}(\{f_i | sr_i = sr_k\})} \quad (2)$$

Where f_i and sr_i are the frequency and sample rate of the i^{th} measurement pair, $i = 1 \dots N$ measurements, $k = 1 \dots m=47$ sample rates, and sr_k is the k^{th} sample rate.

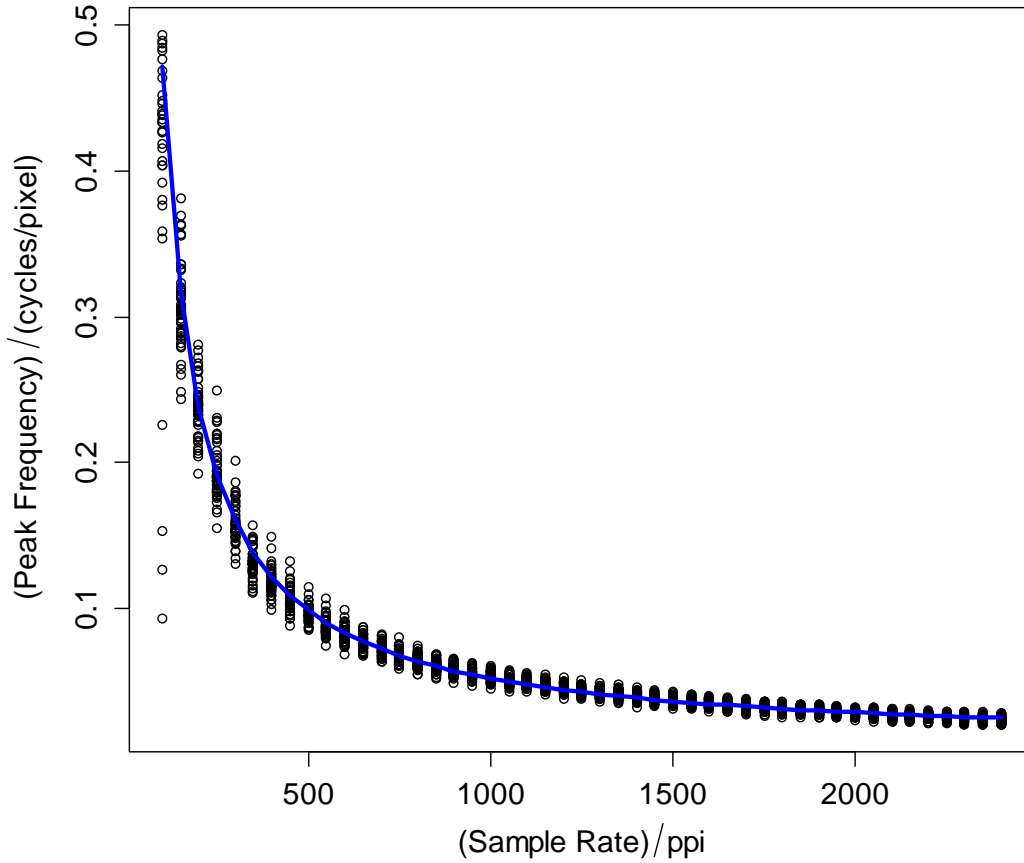


Figure 5 Fitted model predictions plotted over observed data. Frequency measurements are shown in relation to ground truth sample rates.

Figure 5 shows the fitted values plotted over the observed data. Weighted residuals, $\sqrt{w_i}(f_i - (\beta_0 + \beta_1 sr_i))$, plotted as a function of sample rate are shown in Figure 6. The fact that the residuals are evenly distributed around zero indicates the model fits the data fairly well and that the chosen weights effectively equalize the variances of the frequencies at different sample rates. Most of the

remaining structure visible in the residuals is caused by the discretization of the raw data and do not have a significant effect on the final values and uncertainty intervals for unknown images.

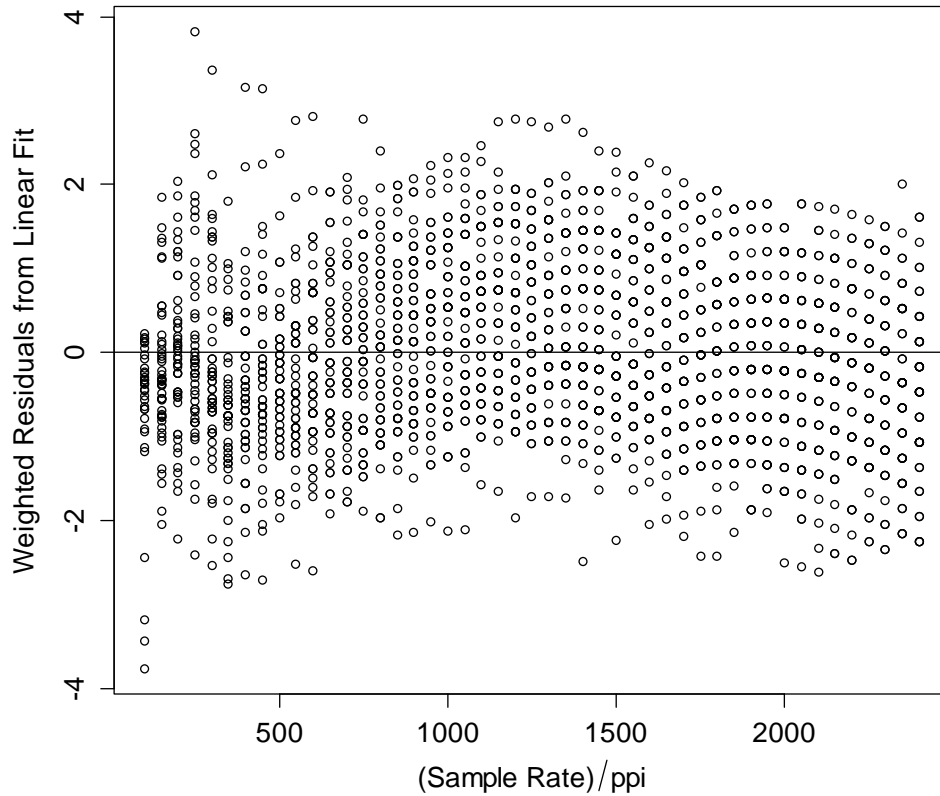


Figure 6 Weighted residuals (observed– predicted frequency)

The parameters of the model in (1) are found to be $\beta_0 = 0.005\ 991$ and $\beta_1 = 46.484\ 416$.

For prediction of sample rate from frequency, we rearrange equation (1) to form the measurement function

$$SampleRate = \frac{\beta_1}{frequency - \beta_0} \quad (3)$$

Thus, to apply the model to fingerprint images of unknown sample rate, we would divide the slope value⁶, $\beta_1 = 46.484416$, by the measured center (peak) frequency of the dominant peak of the spectrum yielded by the SIVV utility minus the intercept value, $\beta_0 = 0.005991$.

3.4. Uncertainty Analysis

The measurement function derived from the linear regression model for the data is then used as the basis for an uncertainty analysis according to [16][17] utilizing an R library created for the purpose [18]. We refer to the uncertainty analysis procedure described in [16][17] as the Guidelines for Uncertainty Measurement, or the GUM. Table 1 lists values and uncertainties on the two model parameters. The expanded uncertainty (**U**) is not a single value, but rather depends upon the position of a given prediction along the fit curve of Figure 5

Table 1 Model parameter values and uncertainties

Source	Value	Uncertainty (u)
Intercept (β_0)	0.005 991	0.000 136 909
β_1	46.484 416	0.180 389 123

On the steeply sloping regions of Figure 5, the value of **U** is relatively small, whereas the uncertainty interval broadens in the flatter regions of the curve. Table 2 illustrates this using a sample of SIVV frequency values, the corresponding predicted sample rate, and the combined expanded uncertainty, **U**, computed using the GUM. The implication of Table 2 is that given a SIVV-measured frequency of a fingerprint image of unknown sample rate, the interval likely to contain the true sample rate with 95 % confidence will lie between $\pm U$ of the sample rate predicted by the measurement function. Thus, we see that given a frequency of 0.05 cycles/pixel, we predict a sample rate of 1056 ppi \pm 164 ppi. A frequency of 0.10 gives us a sample rate prediction of 494 ppi \pm 74 ppi. This latter case is illustrated in Figure 7.

⁶ Note that with sample rate having units of pixels per inch and frequency having units cycles per pixel, β_1 has units cycles per inch and β_0 has units of frequency, i.e., cycles per pixel.

Table 2 Expanded Uncertainty for sample rates predicted by SIVV frequency.

Frequency	Sample Rate	U
0.02	3318	1488.0
0.03	1936.1	364.9
0.04	1366.8	224.6
0.05	1056.2	164.3
0.06	860.7	130.4
0.07	726.2	108.6
0.08	628.09	93.4
0.09	553.33	82.2
0.1	494.47	73.7
0.11	446.93	66.9
0.12	407.73	61.5
0.13	374.85	57.0
0.14	346.88	53.3
0.15	322.79	50.2
0.16	301.83	47.5
0.17	283.43	45.2
0.18	267.14	43.3
0.19	252.62	41.6
0.2	239.6	40.1
0.21	227.85	38.9
0.22	217.21	37.8
0.23	207.51	36.9
0.24	198.64	36.1
0.25	190.5	35.5
0.26	183	35.0
0.27	176.07	34.7
0.28	169.65	34.5
0.29	163.67	34.4
0.3	158.11	34.5

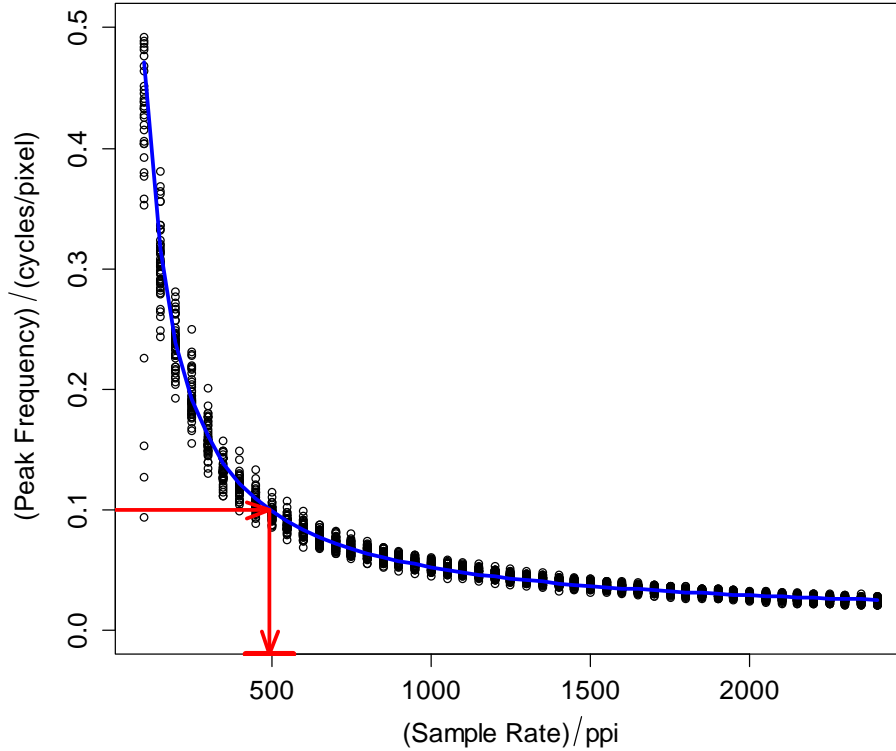


Figure 7 Illustration of prediction of sample rate using the model with $\pm U$ shown as a red bar on the abscissa. The frequency measurements are plotted against the ground truth sample rates.

3.5. Prediction Results

We applied the model to the test fingerprint image dataset described in section 3.1.2. For each of the 2484 images we apply equation (3) to predict a sample rate from the center frequency of the dominant peak. We do not expect the central peak frequency values to map precisely to sample rates, but rather to reach some approximation to the actual sample rate within some tolerance. Hence, we evaluate the accuracy of our model by measuring the proportion of predicted sample rates that differ from actual sample rates within each of a series of thresholds. Thus, we compare absolute differences of observed and predicted sample rates and assign values 1 and 0 as

$$\gamma_i = \begin{cases} 1 & \text{if } |O_i - P_i| \leq \tau_k \\ 0 & \text{if } |O_i - P_i| > \tau_k \end{cases} \quad (4)$$

where O_i , P_i are respectively the ground truth and predicted sample rate of the i^{th} sample, $i = 1 \dots 24770$, and τ_k the k^{th} threshold value, $k=0 \dots 800$. For each of the values, τ_k , we compute the proportion of predictions within the threshold limits as

$$P_k = \frac{\sum_{i=1}^N \gamma_i}{N} \tag{5}$$

where $k=0 \dots 800$ and $i = 1 \dots N=24770$.

Figure 8 exhibits the proportion of cases in which the absolute difference between actual and predicted sample rates are less than each threshold from zero to 800.

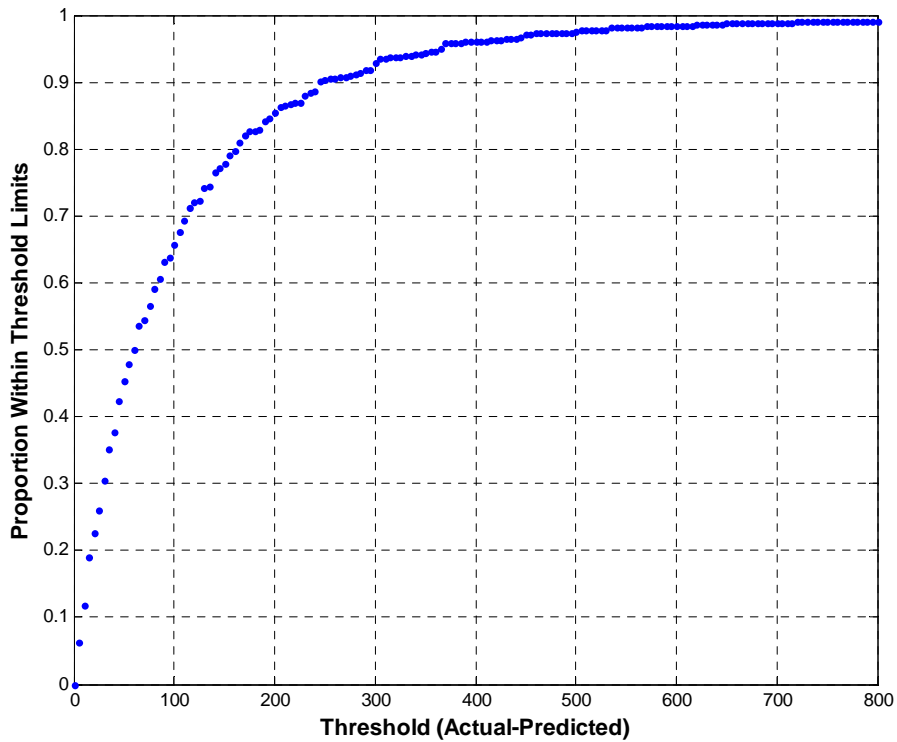


Figure 8 Prediction accuracy within specified error thresholds SD27A cardscan, N= 24 704

Thus, applied to a fingerprint image of unknown sample rate from a population of images similar to the SD27 images used for testing, the SIVV together with an appropriate regression model should be able to estimate the sample rate within ± 100 ppi in 64 % of cases, ± 200 ppi in 84 % of cases, ± 300 ppi in 93 % of cases.

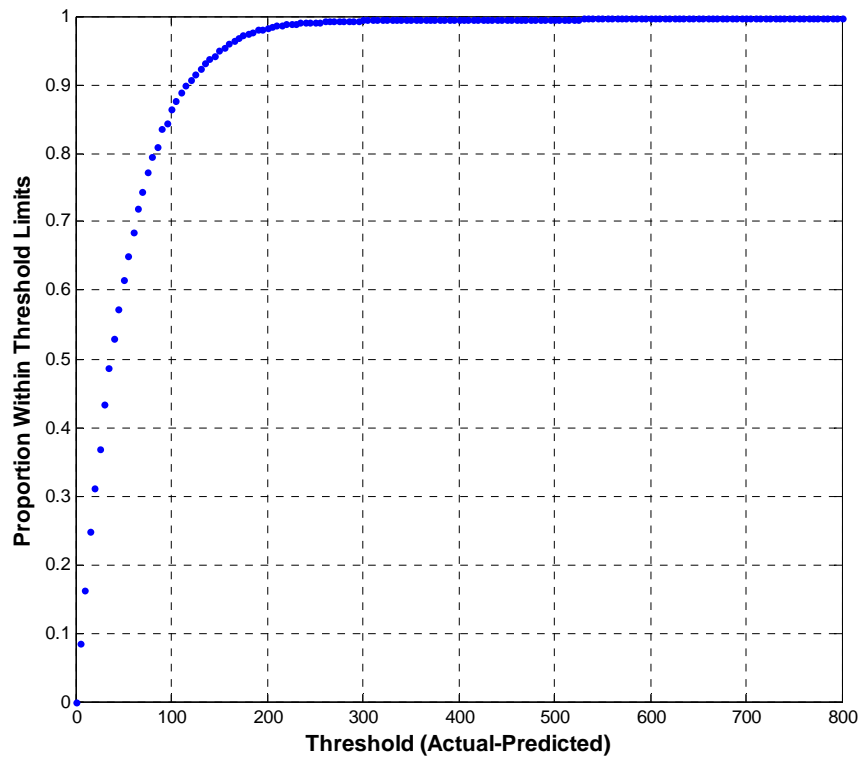


Figure 9 Prediction accuracy within specified error thresholds LAC livescan, N= 23 198

In spite of the fact that the model was developed using cardscan images, the model appears to perform rather well on the livescan images from this population, finding 95 % of the predictions correct within ± 150 of the actual sample rate (see Figure 9). We note that the livescan data contain sample rates only up to 1000 ppi, so in this case the populations used for modeling and testing are definitely not identical. The main point here, however, is that the model developed using cardscan images may be able to be used effectively with some populations of livescan images as well, without modification. For populations of images where the model built on the data used here does not perform adequately as is, it is likely that a similar model could be fit using the procedures outlined here to obtain improved performance.

4. Discussion of Results

Clearly while the simple predictive model derived in the foregoing discussion is not capable of determining the exact image spatial sample rate, it does exhibit utility in classifying the image with an approximate sample rate. Taken together with the measure of combined expanded uncertainty, U , each predicted sample rate may be associated with an interval around the prediction within which the true sample rate should be found with 95 % confidence. In the operational case where the alternative is to guess in trial and error fashion over a range of possible sample rates and transforming a template multiple times until the best match is found, reducing the number of sample rate alternatives could be of at least some, if not substantial, benefit. Using the SIVV-based model described here might reduce the number of trials to

several candidates within the appropriate uncertainty interval of the sample rate predicted by the model. Additionally, this model can be an effective trigger for mitigation actions in the event of a systematic failure of fingerprint image capture and processing pathways.

Use of the model developed here has been demonstrated for a set of card scanned fingerprints and for a set of fingerprints acquired by a liveness device. Additional models may be required for fingerprints acquired via other sensors, such as capacitive, or even contactless devices. Additional work is planned for these modalities.

Note that SIVV processing of the test dataset yielded some failures of the peak-finding algorithm. In 57 of 24 827 SD27A images, the SIVV failed to find a dominant spectral peak. This amounts to 0.23 % of the test fingerprints. As a frequency value of zero would result in a singularity condition for the prediction model, these cases were filtered from the analysis. Various mitigation strategies are being considered to address these failure cases in future updates of the SIVV utility code and/or the manner in which the fingerprints are evaluated via the predictive model.

5. Conclusions

The NIST SIVV utility reveals a dominant spectral peak related to the ridge pattern of fingerprint images. The center frequency of this peak is related to the fingerprint image spatial sample rate. A statistical model may be fitted to SIVV frequency values for fingerprint images digitized over a range of known sample rates in order to develop a predictor function that when applied to the frequency measurement of fingerprint images of unknown sample rate, provides an estimate of the unknown sample rate. Uncertainty analysis of the model via the GUM can provide confidence intervals for predictions of sample rate to further narrow the band of sample rates to be tried in matching the unknown print against exemplars of known sample rate. This estimation can yield several mitigation strategies to help maintain effective matcher performance ranging from initiating corrective strategies at fingerprint capture, implementing corrective resampling action to the image, or transformation of the vector representation of the fingerprint.

6. References

- [1] NIST Special Publication 500-290: “American National Standard for Information Systems — Data Format for the Interchange of Fingerprint, Facial & Other Biometric Information (ANSI/NIST ITL 1-2011)”. Approved November 9, 2011.
- [2] FBI/CJIS, “Electronic Biometric Transmission Specification (EBTS) V. 9.4”, IAFIS-DOC 01078-9.4 Draft, Federal Bureau of Information Criminal Justice Information Services, Clarksburg, WV, August 3, 2012 https://www.fbibiospecs.org/Documents/EBTS_v9.4_Clean_Draft_8.3.2012.pdf. Retrieved 03/11/2013.
- [3] Libert, J. M., Orandi, S., Grantham, J. A 1D Spectral Image Validation/Verification Metric for Fingerprints (NIST IR 7599), National Institute of Standards and Technology, Gaithersburg, MD, 2009, <http://nvlpubs.nist.gov/nistpubs/ir/2009/ir7599.pdf>.
- [4] NIST Biometric Image Software (NBIS) Version 4.2.0 <http://www.nist.gov/itl/iad/ig/nbis.cfm>
- [5] Orandi, S., Libert, J. M., Grantham, J. D., Ko, K., Wood, S.S., Wu, J., “Effects of JPEG2000 Image Compression on 1000 ppi Fingerprint Imagery”, NIST Interagency Report 7778, National Institute of Standards and Technology, Gaithersburg, MD. http://www.nist.gov/customcf/get_pdf.cfm?pub_id=908204. Retrieved 09/01/2012.
- [6] Orandi, S., Libert, J. M., Grantham, J. D., Ko, K., Wood, S. S., Wu, J. C., Petersen, L. M., Bandini, B., “An Exploration of the Operational Ramifications of Lossless Compression of 1000 ppi Fingerprint Imagery”, NIST Interagency Report 7779, National Institute of Standards and Technology, Gaithersburg, MD. http://www.nist.gov/customcf/get_pdf.cfm?pub_id=911122. Retrieved 03/29/2013.
- [7] Orandi, S., Libert, J.M., Grantham, Petersen, L. P., “Effects of JPEG 2000 Lossy Image Compression on 1000 ppi Latent Fingerprint Imagery”, NIST Interagency Report 7780, National Institute of Standards and Technology, Gaithersburg, MD. http://www.nist.gov/customcf/get_pdf.cfm?pub_id=914513. Retrieved 07/31/2013.
- [8] Libert, J. M., Orandi, S., and Grantham, J. D., “Comparison of the WSQ and JPEG 2000 Image Compression Algorithms On 500 ppi Fingerprint Imagery”, NIST Interagency Report 7781, National Institute of Standards and Technology, Gaithersburg, MD. http://www.nist.gov/customcf/get_pdf.cfm?pub_id=910658. Retrieved 03/29/2013.
- [9] Orandi, S., Libert, J.M., Grantham, J.D., Lepley, M., Bandini, B., Ko, K., Petersen, L. P., Wood, S. S., and Harvey, S.G., “Examination of Downsampling Strategies for Converting 1000 ppi Imagery to 500 ppi”, NIST Interagency Report 7339, National Institute of Standards and Technology, Gaithersburg, MD. <http://nvlpubs.nist.gov/nistpubs/ir/2013/NIST.IR.7839.pdf>. Retrieved 03/11/2013.
- [10] Libert, J. M., Orandi, S., Grantham, J.D., “Effects of Decomposition Levels and Quality Layers with JPEG 2000 Compression of 1000 ppi Fingerprint Images”, NIST Interagency Report 7939, National Institute of Standards and Technology, Gaithersburg, MD. <http://nvlpubs.nist.gov/nistpubs/ir/2013/NIST.IR.7939.pdf>. Retrieved 11/18/2013.
- [11] Garris, M. D. and McCabe, R. M. NIST Special Database 27: Fingerprint Minutiae from Latent and Matching Tenprint Images, NIST Technical Report NISTIR 6534 & CD-ROM, June 2000.
- [12] Seber, G. A. F., and C. J. Wild. Nonlinear Regression, Hoboken, NJ: Wiley-Interscience, 1989.
- [13] Wilkinson, G. N. and Rogers, C. E. (1973) Symbolic descriptions of factorial models for analysis of variance. *Applied Statistics*, **22**, 392–9.
- [14] R Core Team (2013). R: A language and environment for statistical computing. R Foundation for Statistical Computing, Vienna, Austria. URL <http://www.R-project.org/>.

- [15] MATLAB Version: 8.1.0.604 (R2013a). Natick, Massachusetts: The MathWorks Inc., 2010.
- [16] Barry N. Taylor and Chris E. Kuyatt (1994). Guidelines for Evaluating and Expressing the Uncertainty of NIST Measurement Results. NIST Technical Note 1297.
- [17] Evaluation of measurement data – Guide to the expression of uncertainty in measurement JCGM 100:2008 (GUM 1995 with minor corrections)
- [18] Stephen L R Ellison. (2014). metRology: Support for metrological applications. R package version 0.9-16.1. <http://CRAN.R-project.org/package=metRology>
- [19] Tukey, J. W. Exploratory Data Analysis. Addison-Wesley, Reading. 1977.
- [20] Galton, F. (2005). *Finger prints*. Mineola, NY: Dover Publications. (Original work published 1892)